11 pages

Magneto-acoustic oscillations directly observed on the sun's surface

Haisheng Ji[1,2,3], Parida Hashim[2], Jiong, Qiu[4], Zhenxiang Hong[1], Zhe, Xu[1,6], Jinhua, Shen[2], Ya, Wang[1], Kaifan Ji[6], Wenda Cao[5], Philip, Goode[5]

1. Purple Mountain Observatory, DMSA/CAS, Nanjing, China
2. Xinjiang Astronomical Observatory, CAS, Urumqi, 830011, China
3. CfASS, China Three Gorges University, Yichang, 443002, China
4. Department of Physics, Montana State University, Bozeman MT, USA
5. Big Bear Solar Observatory, 40386 North Shore Lane, Big Bear City, CA 922314, USA
6. Yunnan Astronomical Observatory, CAS, Kunming, 830011, China

ABSTRACT

In this paper, we report the discovery of 5-minute oscillation for the line of sight magnetic field in the plage beside a solar active region. The finding is a by-product when we try to resolve fine-scale mass and energy flows from the plage region for heating solar corona with high-resolution observations taken with Goode Solar Telescope (GST) at Big Bear Solar Observatory (BBSO). The magnetic oscillations with dominant periods around 5 minutes, are well-correlated with p-mode oscillation of Doppler speed. Both magnetic field and Doppler speed are observed by Helioseismic and Magnetic Imager (HMI) on-board the Solar Dynamic Observatory (SDO). We give an MHD solution for the amplitude of the magneto-acoustic oscillations in the photosphere where gas pressure dominates, showing that the amplitude will be proportional to magnetic field strength. We verify the solution with observations. We further show that the Doppler speed becomes slower in the region of stronger magnetic field strength, an evidence of coupling between kinetic energy and magnetic energy. The coupling also gives anti-phase magnetic oscillations in two kinds of regions with either slower or faster than average Doppler speed, as given by data analysis to the observations. All these show that the phenomena are just magneto-acoustic oscillations on solar surface, the existence of which there is only indirect evidence until now in the literature about the Sun. Our findings give a new diagnostic tool for explore the relationships between magneto-acoustic oscillations and coronal heating, as well as helioseismology.

1. Introduction

The study of oscillations of various modes on the Sun have proven to be very powerful tool to explore the physical nature of our star. Since Leighton et al. (1962) discovered the solar five minutes p-mode oscillations, the study of the oscillations, named as helioseismology, has so far been one of the most successful and magnificent discipline in astrophysics (Basu, 2016). The p-mode oscillations are standing acoustic waves powered by thermal pressure and these waves have provided a unique window into the interior of Sun (Ulrich, 1970). On the other hand, the Sun is a magnetized star, it is naturally anticipated that MHD waves will be excited and they should exist in all layers of solar atmosphere according to the principle of magnetohydynamics (MHD) or plasma physics (Alfvén 1942). However, for a long time, MHD waves had not been observed until high-resolution extreme-ultraviolet (EUV) images on the space missions SOlar and Heliospheric Observatory (SOHO) and Transition Region and Coronal Explorer (TRACE) were available in the late 90s of last century. Since then, there have been a lot of observations of intensity oscillations in coronal loops with periods of $\sim$ 200 - 400 seconds in the visible, EUV, X-ray, and radio wavelengths, and some oscillations are interpreted in terms of helioseismic global 5-min oscillations, or 3-min near sunspots (De Moortel et al. 2000; De Moortel et al. 2002; De Moortel & Nakariakov 2012), some with wave coupling of coronal fast kink mode and photospheric global oscillations (e.g., see reviews by Banerjee et al. 2007; Nakariakov and Verwichte 2005; Nakariakov et al. 2016; Ruderman and Erdelyi 2009; Stepanov et al. 2012; VanDoorsselaere et al. 2016; Wang 2011, 2016 and references therein). These observations have led to a rapid development of coronal seismology with the aim to explore the physical nature of coronal magnetic fields (e.g., Zhang et al., 2017). In addition, there have appeared a new round of interest to investigate the role of waves and oscillations in the heating of solar corona (De Moortel & Nakariakov 2012) and modulation of flare emissions (e.g., Stepanov & Zaitsev 2014, Li et al. 2017).

For coronal heating, an important target for investigation is the footpoint regions of coronal loops, shown as "faculae" on the photosphere or "plage" in the chromosphere. The region is believed to have a stronger heating rate, with prevalent oscillations at various wavebands (De Pontieu et al. 2003; Fletcher et al. 1999). The oscillations usually serve as a piece of indirect evidence of magneto-acoustic waves. By exploring correlations between oscillatory signals observed at different levels, we hope to resolve fine-scale mass and energy flows passing through the chromosphere, the interface layer sandwiched between corona and photosphere (De Pontieu et al. 2014; De Pontieu et al. 2009; Solanki et al. 2003; Aschwanden et al. 2007). We carry out this kind of research for a plage region with high-resolution observations taken at Big Bear Solar Observatory. During the research, we find that periodic mass ejections from the chromosphere are seemingly associated with a periodic weak peaks in the time profile for the flux of line-of-sight magnetic field, which is a signature of coronal heating

powered by magneto-acoustic oscillations (The results are under preparation for a separate paper). The peaks may be the signature that MHD waves could be directly observed on solar surface. Due to the scientific significance, the research was switched to search for magneto-acoustic oscillations in the entire region. It turns out that, in some parts of the plage area, magneto-acoustic oscillations are so obvious that they are cousins of p-mode oscillations of sound speed.

In this Letter, we firstly give a solution for magneto-acoustic waves for the photosphere where thermal pressure dominates from a set of linearized MHD formulations. Unlike previous solutions in literature or textbook (e.g., Priest 2014), our solution predicts the dependence of oscillating amplitude on local magnetic field. In §3, we give and analyze the observed oscillations of the line of sight magnetic field and their association with p-mode oscillations. Conclusion and discussions are given in §4.

2. MHD Formulation

In the photosphere, β value of plasma, the ratio of thermal pressure over magnetic pressure, is much larger than 1. However, the parameter has never been used in derivation of solutions for MHD waves. To understand their behavior, we assume a vertical magnetic field $B_0(x, y)\hat{z}$ and neglect horizontal components to model the line of sight magnetic field B_{los} in the plage region. We start with ideal MHD equations neglecting gravity, viscosity, and diffusion. The momentum and induction equations are given by

$$\rho\left[\frac{\partial}{\partial t} + (\vec{v}\cdot\vec{\nabla})\right]\vec{v} = -\vec{\nabla}P + \frac{1}{\mu_0}(\vec{\nabla}\times\vec{B})\times\vec{B}, \tag{1}$$

$$\frac{\partial\vec{B}}{\partial t} = \vec{\nabla}\times(\vec{v}\times\vec{B}). \tag{2}$$

We then introduce linear perturbations so that $\vec{v} = \vec{v}_1, \vec{B} = B_0\hat{z} + \vec{B}_1, P = P_0 + P_1$, where the subscript "1" indicates perturbed properties. The linearized induction equation and momentum equation are given by

$$\frac{\partial\vec{B}_1}{\partial t} = \frac{\partial\vec{v}_1}{\partial z}B_0 - (\vec{\nabla}\cdot\vec{v}_1)B_0\hat{z} - (\vec{v}_{1\perp}\cdot\vec{\nabla}_\perp)B_0\hat{z}, \tag{3}$$

$$\rho_0\frac{\partial\vec{v}_1}{\partial t} = -\vec{\nabla}\left(P_1 + \frac{1}{\mu_0}B_0B_{1z}\right) + \frac{\partial\vec{B}_1}{\partial z}\frac{B_0}{\mu_0} + \frac{1}{\mu_0}(\vec{B}_{1\perp}\cdot\vec{\nabla}_\perp)B_0\hat{z}, \tag{4}$$

where $\perp$ denotes operation or components in the horizontal direction. In terms of horizontal and vertical components, we can assume that the solutions to Equations (3 - 4) are in the

following form:

$$\begin{cases} \vec{v}_1 = & [\vec{v}_\perp(x,y) + v_z(x,y)\hat{z}]e^{i(k\cdot z-\omega t)} \\ \vec{B}_1 = & [\vec{B}_\perp(x,y) + B_z(x,y)\hat{z}]e^{i(k\cdot z-\omega t)} \\ P_1 = & p(x,y)e^{i(k\cdot z-\omega t)} \end{cases} \tag{5}$$

where k is the wave number of the perturbation in the vertical direction, and ω is the frequency of the wave. Since $\partial\vec{B}_{1\perp}/\partial t = (\partial\vec{v}_{1\perp}/\partial z)B_0$, the perturbed momentum equations for the horizontal components can be re-written as

$$\vec{\nabla}_\perp B_{1z} = -\frac{\mu_0}{B_0}\left[-i\omega\rho_0(1-\frac{v_a^2}{v_p^2})\vec{v}_\perp + \vec{\nabla}_\perp p\right] - B_{1z}\vec{\nabla}_\perp(\ln B_0), \tag{6}$$

where $v_a^2 \equiv B_0^2/(\mu_0\rho_0)$ is the Alfvén speed, and $v_p^2 \equiv \omega^2/k^2$ is the phase speed of the magnetoacoustic wave in z-direction.

Below the chromosphere, the plasma $\beta \gg 1$, the fast-mode wave along the equilibrium field $B_0\hat{z}$ is the sound wave, and its phase speed $v_p^2 = c_s^2 = \gamma p_0/\rho_0$, where γ is the ratio of the specific heats. In this case, the term $v_a^2/v_p^2 = 1/(2\gamma\beta) \ll 1$; therefore, we are left with

$$\vec{\nabla}_\perp B_{1z} = -\frac{\mu_0}{B_0}\left(-i\omega\rho_0\vec{v}_{1\perp} + \vec{\nabla}_\perp p_1\right) - B_{1z}\vec{\nabla}_\perp(\ln B_0). \tag{7}$$

We can re-write the above equation as:

$$\vec{\nabla}_\perp B_{1z} = -\frac{\mu_0}{B_0}\left(\rho_0\frac{\partial\vec{v}_{1\perp}}{\partial t} + \vec{\nabla}_\perp p_1\right) - B_{1z}\vec{\nabla}_\perp(\ln B_0). \tag{8}$$

The above relation describes magneto-acoustic waves with transverse gradient for perturbed magnetic field being included. The first term in the right hand side, the gas speed and pressure perturbations, can be considered as an excitation term for the perturbed magnetic field. In the photosphere, gas pressure dominates the magnetic pressure. That is

$$|\rho_0\frac{\partial\vec{v}_{1\perp}}{\partial t} + \vec{\nabla}_\perp p_1| \ll 1,$$

and we have

$$\lim_{B_0\to 0}(\rho_0\frac{\partial\vec{v}_{1\perp}}{\partial t} + \vec{\nabla}_\perp p_1) = 0,$$

in the photosphere. Thus, we define the first term in the right hand side of equation (8) as

$$-\frac{\mu_0}{B_0}(\rho_0\frac{\partial\vec{v}_{1\perp}}{\partial t} + \vec{\nabla}_\perp p_1) = \vec{W}(x,y)e^{i(kz-\omega t)}. \tag{9}$$

We see that the perturbed field B_{1z} vanishes when this source term $\vec{W}(x,y)$ is zero. Not to lose generality, we may approximate the local geometry to circular cylindrical flux tubes

of azimuthal symmetry (e.g. the $m = 0$ sausage mode), then the solution of the perturbed magnetic field is given by

$$B_{1z} = B_0^{-1}\left[C + \int B_0 W dr\right] e^{i(kz-\omega t)}, \tag{10}$$

where r represent the transverse dimension, being equivalent to $s_\perp$ in the Letter. C is a constant from the integral. Recall that $B_{1z} = 0$ when $W = 0$, we get $C = 0$. In the end, the perturbed magnetic field is given by

$$B_{1z} = \left[B_0^{-1}\int B_0 W dr\right] e^{i(kz-\omega t)}. \tag{11}$$

We see that $W(x, y)$ is a function ~~which~~ that describes the degree of deviation of magnetized plasma in the photosphere from non-magnetized one (pure gas). For pure gas $W(x, y) = 0$, which says that the perturbed sound speed is only produced by perturbing thermal pressure. In the photosphere, the presence of magnetic field itself will be perturbed by the perturbing thermal pressure as well, and thus produce a non-zero value for W(x, y). Therefore, W(x, y) will depends weakly on the magnetic field. Thus, solution (11) predicts that the oscillation amplitude should be larger in regions with the stronger magnetic field as background. However, it will not be applicable to the region of sunspot where plasma β becomes much smaller than quiet regions.

3. Observation and results

We use Doppler velocity map and magnetograms from Helioseismic and Magnetic Imager (HMI) (Schou et al. 2012) on-board Solar Dynamic Observatory (SDO) (Pesnell et al. 2012) in this research. HMI observes the full disk Sun in the Fe I absorption line at 6173 Å to measure oscillations of sound speed and the magnetic field in the photosphere. The oscillation measurements are used for helioseismic studies of the solar interior, while the magnetic-field measurements are for studies of solar activity. The sequence of co-aligned HMI Dopplergrams is analyzed to track the line-of-sight velocity signals in different locations of the active region. The Dopplergrams here used is calibrated with most of the observer motion effects and solar-rotation signal removed.

The data analyzed in this research is near the active region NOAA 11259. On July 22, 2012, the region was observed with narrow band imaging (bandpass 0.05 nm) at He I 1083 nm with the GST at BBSO (Goode et al. 2010; Cao et al. 2010). The time period corresponds to day time of BBSO, lasted over 4 hours. A previous study has revealed

dynamical events originating in intergranular lane areas and subsequently lighting up the corona from their origin in the photosphere on through to their brightening of the local corona (Ji Cao and Goode 2012). The active region belongs to β-type with a leading sunspot of negative magnetic polarity. Figure 1 gives a sample magnetogram covering the active region with the size of 150 arcsec × 150 arcsec.

To search for possible oscillations of magnetic field, we divide the whole region in Figure 1 into 10×10 sub-areas and get the time profile for the net magnetic flux in each sub-area with de-rotated magnetograms. In all, at least 44 sub-areas can be selected for the appearance of oscillatory signature on the light curves of these sub-areas. For the purpose of this study, we excludes the regions covering the sunspot, where thermal pressure is no longer dominate over magnetic pressure, and the regions with mixed polarity, where variation of magnetic field could be mixed with small-scale magnetic activities, like magnetic cancelling.

Figure 2a gives a time profile for the mean magnetic field inside the sub-area labeled 37 in Figure 1. Over its slowly varying component, there are quasi-periodic oscillatory signals. Wave trains persistently appear throughout the time period. To make the oscillatory components clearer, Figure 2b gives its time profile with background being subtracted. Even with simple visual inspection, it shows that the oscillatory components has a period of about 5 minutes. Wavelet analysis confirms that the dominant periods are of the order of 300 seconds (Figure 2c). To compare the magnetic oscillations with the global p-mode oscillations, Figure 4b-c gives time profiles of mean upward speed (blue shifted) in the same sub-area. We see that most of the oscillatory peaks of magnetic field are synchronized with peaks of either peaks or valleys of the oscillating speed. In addition, power spectrum for the global p-mode oscillations given in panel (e) is basically conformable with that of magnetic oscillation.

For all sub-areas labeled in Figure 1, mean magnetic strength varies at least up to one order of magnitude. So the magnetic deviation $W(x, y)$ as defined in equation (9) is different from one sub-area to another. This will result in different oscillatory amplitudes according to equation (11). Since both amplitude and magnetic strength vary with time, we measure averaged oscillating amplitude and magnetic field strength in each sub-area. For the sub-area 37, the results are about 1.48 G for mean oscillating amplitude and 209.8 G for mean magnetic field strength, respectively (see Figure 2b). A scatter plot for all oscillating amplitudes and magnetic field strength from all labeled sub-areas is shown in Figure 3. We see that a linear relationship can be obtained and we see that the oscillating amplitude is larger with stronger magnetic field. Observations have confirmed the prediction made by equation (11).

Note that oscillating amplitude is about 0.5% in overall, which is very small indeed. Therefore, one thing we should worry about is that the tiny magnetic oscillation is a pseudo

result produced by the Doppler shifting of line center that will affect inferring of magnetic field. In an effort to exclude this possibility, we discover that, on average, both oscillating amplitude and magnetic field strength are larger in those pixels with smaller Doppler speed. Again, taking sub-area 37 as a sample for demonstration. We obtain two kinds of time profiles for magnetic field strength, one is for those pixels with larger Doppler speed while another is associated with smaller Doppler speed. A result is given in Figure 4, in which time profiles in upper and lower panels are associated with Doppler speed larger than 450 ms^{-1} and smaller than 250 ms^{-1}, respectively. It shows that stronger magnetic field is associated with slower Doppler speed. In Figure 4, we can further see that the two time profiles ~~are in anti-phase relationship consistently~~. This gives us following picture: the two kinds of regions take turns ~~to~~ have magnetic concentration and lessening periodically.

4. Conclusions and discussions

In ~~the~~ Letter, we report magneto-acoustic oscillations directly observed on solar surface, the photosphere. ~~The~~ conclusion is ~~made~~ based on both observation and theoretical MHD modeling to the coupling between perturbations of velocity and magnetic field in the photosphere where thermal pressure dominates magnetic pressure. Observation shows that magnetic field strength contains quasi-periodic oscillatory signals with the dominant periods ~~that are~~ of the order of 5 minutes. The oscillation is apparently correlated with the global p-mode oscillations. We have provided following two proofs to verify that the phenomenon is just magneto-acoustic oscillations.

1) With a solution for oscillation amplitude from linearized MHD formulations for the photosphere, we show that it will be larger in the regions of stronger magnetic field where magnetized plasma ~~have~~ a larger deviation from pure gas. A statistics from a number of sub-areas gives a linear positive relationship between the oscillation amplitude and field strength, confirming the solution.

2) In the regions with slower Doppler speed, magnetic field is stronger and oscillation amplitude is larger than in those regions with larger Doppler speed. As stated in the solution in §2, magneto-acoustic oscillations will be stronger in strongly magnetized regions, and thus more local kinetic energy is converted to the oscillations. In this case, we should expect smaller Doppler speed. On the other hand, larger Doppler speed is associated with ~~weekly~~ magnetized plage region. We further discovered that the magneto-acoustic oscillations in the two regions are persistently ~~in anti-phase~~ throughout the whole time period. This gives us an interesting picture for magneto-acoustic oscillations in the photosphere: the two kinds of regions take their turn ~~to~~ have magnetic strengthening and weakening ~~periodically~~. The

phenomenon is quite conformable with the picture of a longitudinal sound wave. In addition, the nice wave picture makes us believe that the magneto-acoustic oscillations reported in this Letter are not pseudo-results caused by the Doppler shifting of line center, which can affect inferring of magnetic field from polarization signals.

Since photospheric magneto-acoustic oscillations can leak into the chromosphere and corona, the coronal waves studied in coronal seismology can be traced back to their photospheric source. In this way, coronal seismology will be connected with traditional helioseismology. The photospheric magneto-acoustic oscillations will be much useful for studying coronal heating in the plage region to see whether it is powered by magneto-acoustic oscillations. As for the specific physical heating mechanism, the magneto-acoustic disturbances may evolve into upward propagating shocks (Hansteen et al. 2006; van der Voort et al. 2016) or they may even modulate ongoing small-scale magnetic reconnection (Chen & Priest 2006). Future spectro-polarimetry observations with higher resolution and high-cadence for the interface layer will help to determine which mechanism is working on.

We thank team SDO/AIA, SDO/HMI for providing the valuable data. SDO is a NASA project. The HMI data are downloaded via the Virtual Solar Observatory and the Joint Science Operations Center. This work is supported by NSFC grants 11790302, 11729301, 11773061, 11773072 and 11873027. W. Cao and P. R. Goode acknowledge the support AFOSR-FA9550-19-1-0040 and NASA-80NSSC20K0025 grants.

REFERENCES

Alfvén, H. 1942, Nature, 150, 405

Aschwanden, M. J., Winebarger, A., & Tsiklauri, D. et al. 2007, ApJ, 659, 1673

Banerjee, D., Erdélyi, R., & Oliver, R., et al. 2007, Sol. Phys., 246, 3

Basu, S. 2016, Living Reviews in Solar Physics, 13, 2

Cao, W., Gorceix, N., & Coulter, R., et al. 2010, Astronomische Nachrichten, 331, 636

Chen, P. F. & Priest, E. R. 2006, Solar Physics, 238, 313

De Pontieu, B., Erdélyi, R., & de Wijn, A. G. 2003, ApJ, 595, L63

De Pontieu, B., McIntosh, S. W., Hansteen, V. H., & Schrijver, C. J. 2009, ApJ, 701, L1

De Pontieu B., Title, A. M., & Lemen, J. R. et al. 2014, Sol. Phys., 289, 2733

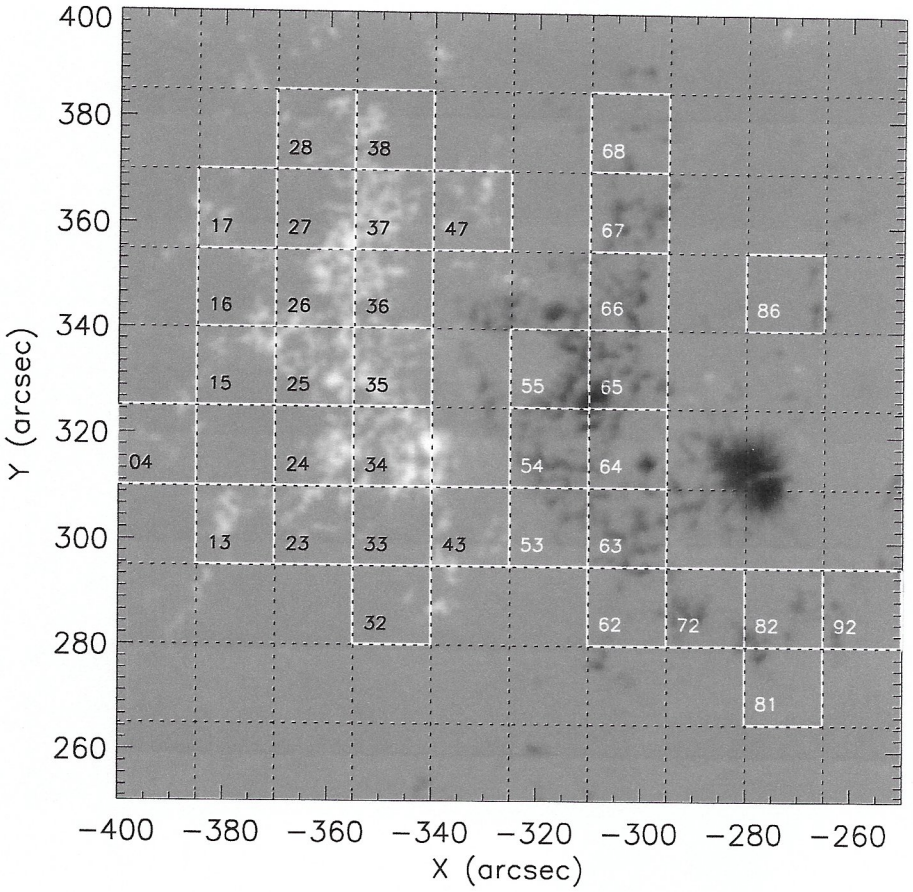

Fig. 1.— A sample magnetogram showing the general magnetic configuration and the 10×10 sub-areas divided for obtaining time profiles.

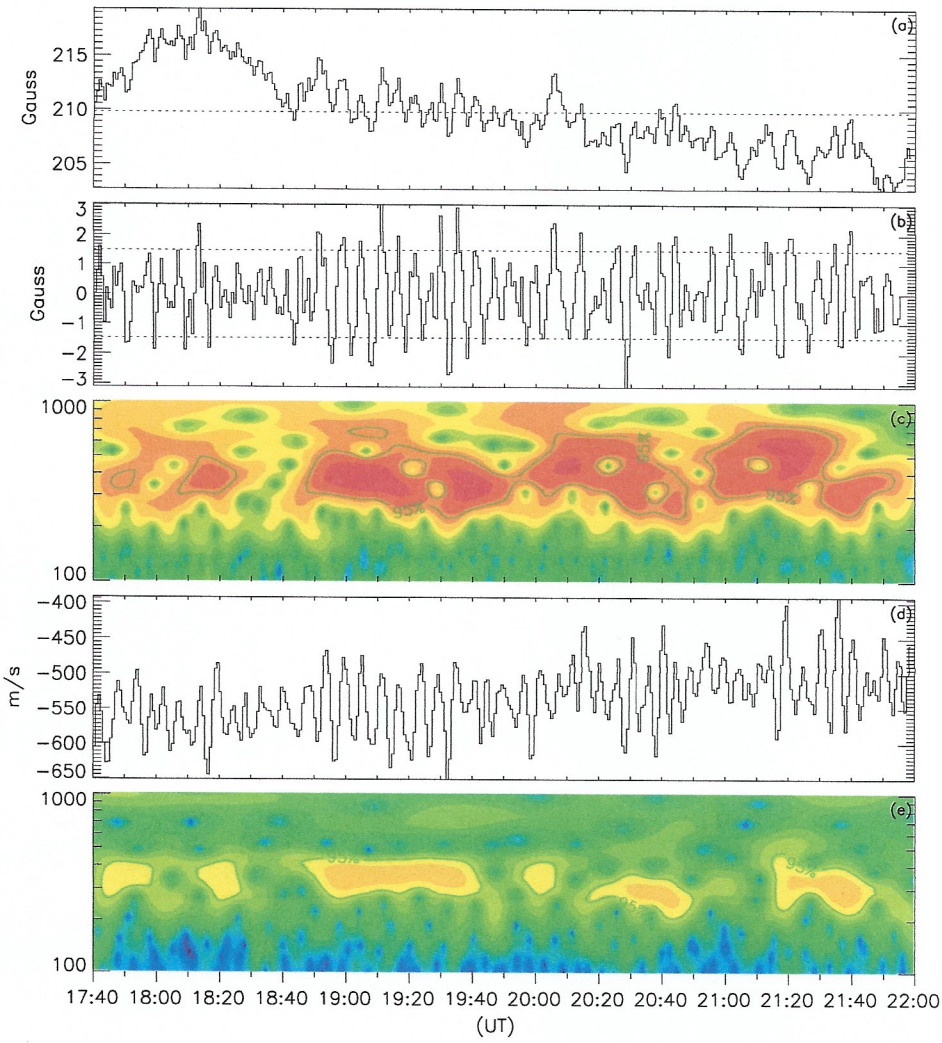

Fig. 2.— An example showing magneto-acoustic oscillations in the sub-area 37 in Figure 1. a) Time profile of magnetic flux showing the general evolution trend. b) A train of oscillatory components obtained from the time profile in panel (a) by subtracting slowly varying component (smoothed one). c) The power spectra of wavelet analysis carried out for oscillatory components in panel (b). c-d) Time profile of Doppler speed (blue shifted) and its power spectrum.

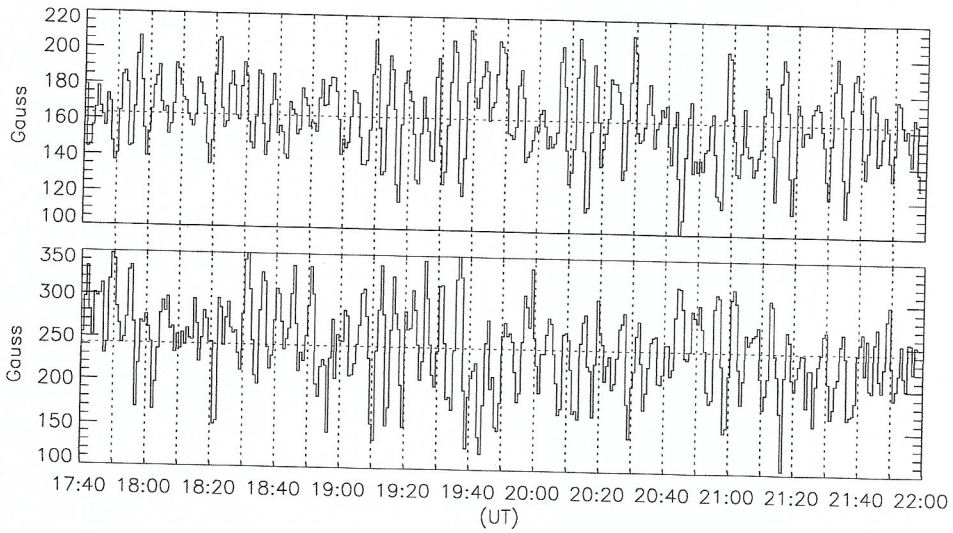

Fig. 4.— Dividing magneto-acoustic oscillations in the sub-area 37 into two classes according to the magnitude of sound speed. Upper panel: time profile for magnetic field averaged over pixels with sound speed larger than 450 ms^{-1}. Lower panel: time profile for magnetic field averaged over pixels with sound speed lower than 150 ms^{-1}. Vertical lines is plotted to help readers to see the persistent anti-phase relationship of the two time profiles. Two horizontal lines give the mean magnetic strength averaged over time. Also note different scales for the two vertical axises.